BAREKENG: Journal of Mathematics and Its Applications
September 2026 Volume 20 Issue 3 Page 2117-2130
P-ISSN: 1978-7227 E-ISSN: 2615-3017
https://doi.org/10.30598/barekengvol20iss3pp2117-2130

FRACTIONAL MATHEMATICAL MODELLING OF THE CORROSION RATE OF ALUMINUM 5083 IN A MARITIME ENVIRONMENT

Muhammad Rifki Nisardi [1*], **Nur Rahmi** [2], **Muhammad Arkam Arifuddin** [3], **Hartina Husain** [4], **Kusnaeni** [5]

[1,3]*Metallurgical Engineering Department, Institut Teknologi Bacharuddin Jusuf Habibie*
[2]*Mathematics Department, Institut Teknologi Bacharuddin Jusuf Habibie*
[4]*Data Science Department, Institut Teknologi Bacharuddin Jusuf Habibie*
[5]*Naval Engineering Department, Institut Teknologi Bacharuddin Jusuf Habibie*
Jln. Balaikota No.1 Parepare, South Sulawesi, 91122, Indonesia

*Corresponding author's e-mail: * **muhammadrifkinisardi@ith.ac.id***

Article Info

Article History:

Received: 31st July 2025
Revised: 21st December 2025
Accepted: 7th March 2026
Available online: 8th April 2026

Keywords:

Aluminum 5083;
Corrosion model;
Fractional Caputo Derivative;
PECE-PI.

ABSTRACT

Aluminum 5083 is one of the materials used for the construction of ship hulls due to its classification as a material with good corrosion resistance. Despite its high corrosion resistance, Aluminum 5083 remains susceptible to galvanic corrosion and pitting corrosion caused by marine environmental conditions. This study develops a mathematical model by adding chloride and passivation effects using fractional differential equations to describe the corrosion rate of Aluminum 5083. The model construction using a Fractional Differential Equation System (FDES) aims to capture memory effects to represent the complex corrosion dynamics accurately. Stability analysis of the fractional model shows that the system is locally asymptotically stable, with all eigenvalues satisfying the condition $|\arg(\lambda_j)| > \frac{\alpha\pi}{2}$. *Furthermore, a numerical solution approach using the PECE-PI method is employed to solve the model, demonstrating agreement between the simulation results and real-world corrosion phenomena. Involvement of different fractional orders α reveals an effect on the rates of increase and decrease in concentration for each variable. The smaller the value of fractional order α, the slower the concentration change process occurs.*

How to cite this article:

M. R. Nisardi, N. Rahmi, M. A. Arifuddin, H. Husain, and Kusnaeni, "FRACTIONAL MATHEMATICAL MODELLING OF THE CORROSION RATE OF ALUMINUM 5083 IN A MARITIME ENVIRONMENT", *BAREKENG: J. Math. & App.*, vol. 20, no. 3, pp. 2117-2130, Sep, 2026.

Journal homepage: *https://ojs3.unpatti.ac.id/index.php/barekeng/*
Journal e-mail: *barekeng.math@yahoo.com; barekeng.journal@mail.unpatti.ac.id*

Research Article · **Open Access**

1. INTRODUCTION

The application of aluminum metal is widely prevalent across various sectors such as electrical engineering, chemistry, building construction, and as a primary material in transportation. This broad usage is attributed to aluminum being a lightweight metal that offers excellent durability, ductility at low temperatures, and high corrosion resistance in environmental exposure. In the maritime sector, aluminum is extensively utilized as a main material for ship hulls in both commercial and defense vessels [1], [2]. One particular grade, Aluminum 5083, is commonly employed in the maritime industry for ship construction due to its favorable combination of corrosion resistance, mechanical strength, and low weight. Although Aluminum 5083 has excellent corrosion resistance due to its Mg–Mn oxide layer, exposure to chloride-rich seawater can still cause localized pitting and galvanic corrosion. Neglecting this issue can adversely impact the material's service life and increase maintenance and repair costs for ships [3]. Modelling the corrosion rate of Aluminum 5083 is a crucial aspect for investigating the material degradation problem, enabling more accurate estimations and effective mitigation strategies. Several researchers have developed mathematical models addressing corrosion rate in metals [2], [4], [5]. However, these existing models are based solely on integer-order differential equations, which inherently possess local limitations and do not incorporate historical effects or long-term memory dependencies within the system [6].

Prior studies have attempted to model the corrosion rate of aluminum materials. Agustini, Fitriah, and Fahrurrorzi (2023) discussed corrosion modeling based on the inhibitors by dividing their model into two types: one without inhibitors and one with inhibitors. They employed three main variables, metal molarity (L), metal transition molarity (N) and corrosion products (K) with an additional compartment inhibitors (I) depending on the types of models. [4]. Subsequently, Maghfiroh, Dewi, and Khusniah (2024) focused on corrosion rate modeling by considering environmental factors that accelerate corrosion. They involved four compartments on the model, metal molarity (L), metal transition molarity (N), corrosion products(K), and the environment molarity(X). The finding of this work is that the molarity of the corroded species stabilizes more rapidly in accelerated corrosion environments [5]. Finally, Fajri et al. [2] developed a mathematical model describing the corrosion rate of Aluminum 5083 used in 60-meter fast missile boats as a strategic defense asset in Indonesia. Their model included four primary compartments: aluminum molarity (L), corrosive ion molarity (N), corrosion products(K), and oxygen (O). Nevertheless, these studies still utilized classical differential equations and have not adopted fractional calculus-based models to describe metal corrosion rates.

In maritime environments, metal corrosion rates depend not only on current conditions but also on prior exposure to corrosive environments. Corrosion processes tend to exhibit non-Markovian characteristics, indicating dependence on past states, and may demonstrate anomalous dynamics such as decelerated or accelerated corrosion rates over time due to accumulated micro-damage. Since corrosion depends not only on current environmental conditions but also on the history of exposure, fractional models can better describe this time-dependent behavior. Given fractional models' capacity to capture memory effects and hereditary properties, they present promising potential in addressing corrosion rate problems in metallic materials. Fractional-order modeling has increasingly advanced and has found applications across diverse fields, including engineering [7], [8], [9], chemistry [10], biology [11], and physics [12]. Fractional-order mathematical models, based on non-integer calculus, offer significant advantages by incorporating memory and hereditary effects, thus providing a more realistic and nuanced representation of corrosion dynamics than classical models. Therefore, this study aims to develop and analyze fractional-order mathematical models of corrosion rate dynamics of Aluminum 5083 in maritime environments. This study only focuses on numerical simulation to identify the behaviors of each compartment without laboratory experiments.

2. RESEARCH METHODS

2.1 Theoretical Review

2.1.1 Corrosion Problem

Corrosion is a commonly occurring reaction process in the environments around us. It is defined as the degradation of metal caused by electrochemical reactions between the metal and its surrounding environment [5]. The phenomenon of metal layer degradation during corrosion results in a decline in mechanical properties,

which adversely affects the material's durability and consequently its safety. Additionally, this process frequently leads to economic losses that require careful consideration by various industrial sectors [13]. Several common types of corrosion frequently encountered include galvanic corrosion, atmospheric corrosion, and pitting corrosion. Galvanic corrosion arises from the difference in electrode potentials between two different metals, whereas atmospheric corrosion occurs due to exposure to air and humidity. Pitting corrosion is a localized form that can cause severe material penetration [14], [15], [16].

Environmental factors such as the presence of oxygen, chloride ions, pH, and temperature significantly influence the corrosion rate [3]. One of the most familiar environments prone to corrosion is seawater due to its high chloride ion content, which acts as a primary factor accelerating corrosion rates. Moreover, humidity, dissolved oxygen, and temperature conditions in marine environments also contribute to the intensive progression of corrosion processes, especially in metals like aluminum and steel [17]. Therefore, a thorough understanding of corrosion mechanisms and their causative factors is essential for developing effective mitigation strategies. In this context, accurate mathematical models for predicting and controlling corrosion serve as vital tools for anticipating material degradation and designing protective measures.

2.1.2 Aluminum 5083

Aluminum 5xxx series alloys exhibit high strength and corrosion resistance, making them widely used in marine vessel materials, automotive components, and industrial applications. Furthermore, Aluminum 5xxx alloys demonstrate superior strength compared to other aluminum alloys due to solid solution strengthening by magnesium, which is one of the primary additive elements [18]. Another research reported that the magnesium content added to aluminum correlates directly with its mechanical properties. In extreme environments, Aluminum magnesium (Al-Mg) alloys are susceptible to stress corrosion cracking and intergranular corrosion [19]. However, the natural formation of a protective oxide layer on the surface of 5xxx series aluminum inhibits the progression of corrosion. In addition to corrosion resistance, these materials are lightweight, contributing to energy efficiency, particularly in marine vehicle construction. This advantage is especially notable in Aluminum 5083, whose tensile strength can reach up to 300 MPa. Regarding corrosion mechanisms, the Magnesium-Manganese (Mg-Mn) oxide layer in the 5083 alloy demonstrates self-healing properties, with a corrosion rate of approximately 0.002 mm/year according to ISO 9227 testing standards.

2.1.3 Fractional Calculus

In this section, we recall definitions related to Caputo fractional derivative needed for the study of the main result to represent memory effects in the system.

Definition 1. Caputo Fractional Derivative [20]

Suppose $\alpha > 0, t > 0$ *and* $n \in \mathbb{N}$. *Caputo Fractional Derivative* ${}_0^C D_t^\alpha := \frac{d^\alpha}{dt^\alpha}$ *with fractional order* α, *for function* $f(t)$ *is defined by:*

$$ {}_0^C D_t^\alpha f(t) = \begin{cases} \dfrac{1}{\Gamma(n-\alpha)} \displaystyle\int_0^t (t-x)^{n-\alpha-1} f^{(n)}(x)\, dx, & n-1 < \alpha < n, \\ f^{(n)}(t), & \alpha = n. \end{cases} \tag{1} $$

Definition 2. The Mittag-Leffler Function [21]

The one-parameter Mittag-Leffler function is expressed as:

$$ E_\alpha(\lambda, z) = E_\alpha(\lambda z^\alpha) = \sum_{k=0}^{\infty} \lambda^k \frac{z^{\alpha k}}{\Gamma(\alpha k + 1)}, \quad (0 \neq \lambda \in \mathbb{R}, z \in \mathbb{C}; Re(\alpha) > 0). \tag{2} $$

2.1.4 Stability Analysis for Fractional Model

Theorem 1. Local stability of fractional differential equation system [20], [22].

Let ${}_a^C D_t^\alpha \boldsymbol{x}(t) = f(\boldsymbol{x}), 0 \leq \alpha < 1$, *and* $\boldsymbol{x} \in \mathbb{R}^n$ *are nonlinear fractional differential equation system. The equilibrium point* $\bar{\boldsymbol{x}}$ *is the solution of* $f(\boldsymbol{x}) = 0$. *The equilibrium point* $\bar{\boldsymbol{x}}$ *is locally asymptotically stable if for all the eigenvalues* λ_j *of the Jacobian matrix evaluated at the equilibrium point* $\bar{\boldsymbol{x}}$ *satisfy* $\left| arg\,(\lambda_j) \right| > \frac{\alpha\pi}{2}, j = 1,2,\dots,n.$

Theorem 2. Routh-Hurwitz criterion for fractional order [23].

The equilibrium point $\bar{x}$ is said to be locally asymptotically stable if it satisfies the term as follows

i. *For $n = 1$ then $|arg\,(\lambda_i)| > \frac{\alpha\pi}{2}$, if $\alpha_1 > 0$.*

ii. *For $n = 2$ then $|arg\,(\lambda_i)| > \frac{\alpha\pi}{2}, i = 1,2$ if it satisfies*

a) $D(p) > 0, a_1 > 0, a_2 > 0$ *or*

b) $D(p) < 0, a_1 < 0$ *and* $\left|tan^{-1}\frac{\sqrt{4a_2 - {a_1}^2}}{a_1}\right| > \frac{\alpha\pi}{2}$.

where $D(p)$ is the discriminant of the polynomial characteristic equation.

iii. *For $n = 3$ then $|arg\,(\lambda_i)| > \frac{\alpha\pi}{2}, i = 1,2,3$ if it satisfies*

a) $D(p) > 0, a_1 > 0, a_3 > 0, a_1 a_2 > a_3$ *for all* $0 \le \alpha < 1$ *or*

b) $D(p) > 0, a_1 \ge 0, a_2 \ge 0, a_3 > 0, \alpha < \frac{2}{3}$ *or*

c) $D(p) < 0, a_1 > 0, a_2 > 0, a_1 a_2 = a_3$, *for all* $0 \le \alpha < 1$.

iv. *For $n > 3$ if $\Delta_1, \Delta_2, \dots, \Delta_n$ is the Routh-Hurwitz determinant*

$$\Delta_1 = a_1,\ \Delta_2 = \begin{vmatrix} a_1 & 1 \\ a_3 & a_2 \end{vmatrix},\ \Delta_3 = \begin{vmatrix} a_1 & 1 & 0 \\ a_3 & a_2 & a_1 \\ a_5 & a_4 & a_3 \end{vmatrix}, \dots .$$

If the following condition is satisfied

$$\Delta_i > 0, i = 1,2,\dots,n-2,$$
$$a_n > 0,\quad \Delta_{n-1} = 0.$$

Then, that is a sufficient condition to claim that $|arg\,(\lambda_i)| > \frac{\alpha\pi}{2}$ for all $\alpha \in [0,1)$.

2.1.5 Predictor-Corrector Product Integration Rule (PECE-PI)

We employ the Predictor-corrector (PECE) with Product Integration (PI) rules method developed by Garrappa [24] in MATLAB to perform numerical simulation for several values of fractional order α. It aims to analyse the dynamical behaviour of the system. By using the PECE-PI method, we get the numerical expression as follows:

$$x_{i_n}^{p} = T_{m-1}[x_i; t_0](t_n) + h^{\alpha}\sum_{j=0}^{n-1} b_{n-j-1}^{(\alpha)} g_i\left(t_j, x_{i_j}\right), \tag{3}$$

$$x_{i_n} = T_{m-1}[x_i; t_0](t_n) + h^{\alpha}\left(\tilde{a}_n^{(\alpha)} g_i(0) + \sum_{j=1}^{n-1} a_{n-j}^{(\alpha)} g_i\left(t_j, x_{i_j}\right) + a_0^{(\alpha)} g_i\left(t_n, x_{i_n}^{p}\right)\right), \tag{4}$$

where $i = 1,2,\dots 6$, $b_n^{(\alpha)} = \frac{((n+1)^{\alpha} - n^{\alpha})}{\Gamma(\alpha+1)}$, $\tilde{a}_n^{(\alpha)} = \frac{(n-1)^{\alpha+1} - n^{\alpha}(n-\alpha-1)}{\Gamma(\alpha+2)}$, and

$a_n^{(\alpha)} = \begin{cases} \frac{1}{\Gamma(\alpha+2)}, & n = 0, \\ \frac{(n-1)^{\alpha+1} - 2n^{\alpha+1} + (n+1)^{\alpha+1}}{\Gamma(\alpha+2)}, & n = 1,2,\dots \end{cases}$, while $\Gamma(\cdot)$ is notation for the gamma function.

2.2. Research Methodology

This research consists of several stages. The first stage begins with a literature review through scientific articles related to the corrosion process occurring in aluminum metal and the influencing factors on the corrosion rate, particularly in maritime environments. The mathematical model developed is an extension of the model previously proposed by [2], in which the prior model considered four variables: aluminum

concentration (L), corrosive ion concentration (N), corrosion product (K), and oxygen (O). This research incorporates two additional variables involved in the aluminum corrosion process in marine environments, namely, chloride ion concentration (C) and the passivation layer concentration (P) as follows:

$$\frac{dL}{dt} = -f(P)[k_1 LN + k_2 LO + k_7 LC], \tag{5}$$

$$\frac{dN}{dt} = k_3 L - k_4 N - k_5 LN, \tag{6}$$

$$\frac{dK}{dt} = k_6 NL - k_{11} K, \tag{7}$$

$$\frac{dO}{dt} = \widetilde{D}_0 (O_{env} - O) - k_{12} LO, \tag{8}$$

$$\frac{dC}{dt} = \widetilde{D}_c (C_{env} - C) - k_{13} LC - k_{10} CP, \tag{9}$$

$$\frac{dP}{dt} = k_8 LO - k_9 P - k_{10} CP\,. \tag{10}$$

The initial conditions applied are as follows

$$L(0) = L_0, N(0) = N_0, K(0) = K_0, O(0) = O_0, C(0) = C_0, P(0) = P_0.$$

Eq. (5) denotes the rate of change of aluminum concentration. The aluminum concentration decreases due to its reaction with corrosive ions. This reaction rate is proportional to the product of the aluminum concentration (L) and corrosive ion concentration (N), as indicated by the coefficient k_1. The multiplicative effect implies a parallel reaction mechanism requiring the presence of both reactants simultaneously. A higher concentration of N and L leads to an increased aluminum consumption rate. Besides corrosive ions, aluminum also reacts with oxygen and chloride ions. However, the reaction with oxygen results in a protective process known as passivation.

Briefly, passivation is the formation of a thin, dense aluminum oxide layer on the metal surface, serving to protect against further corrosion. This process occurs naturally upon aluminum's exposure to oxygen or may be accelerated via chemical or electrochemical treatments [25]. The protective effect is expressed by the function: $f(P) = \frac{1}{1+\varepsilon P}$, where ε denotes the protective effectiveness per unit thickness of the passive layer, and P represents the concentration (thickness) of this layer. This function appropriately models the nonlinear inhibitory effect of the passive layer on the corrosion rate.

Eq. (6) reflects the variation in corrosive ion concentration, which increases due to release from the reaction with aluminum. Conversely, the corrosive ion concentration decreases for two reasons: consumption in corrosion product formation, denoted by the term $k_5 NL$, and loss via decay or side reactions, represented by $k_4 N$. Eq. (7) indicates the rate of accumulation of corrosion products formed by the reaction of corrosive ions and aluminum. Higher levels of N and L correspond to the faster accumulation of K. In addition, corrosion product concentration decreases through natural degradation, represented by $k_{11} K$.

On the other hand, Eqs. (8) and (9) represent the oxygen concentration and the chloride ion change, respectively. In terms of oxygen, it increases through a diffusion process assumed to be linear and proportional to the concentration gradient. This gradient is simplified as the difference between the oxygen concentration in the external environment (O_{env}) and the system (O). Oxygen decreases due to consumption in the reaction with aluminum. In Eq. (9) represents the chloride ion concentration change in the marine environment, and $\widetilde{D}_c$ as the diffusion constant. The chloride concentration decreases because of its reaction with aluminum and consumption related to the protective effect of the passivation layer. Eq. (10) is defined as the passivation concentration. This equation represents the accumulation of the passive layer due to the reaction of aluminum exposed to oxygen, producing a thin oxide (Al_2O_3) layer that protects the metal from corrosion. The passive layer concentration decreases due to natural degradation and consumption, as it protects against corrosive ions.

Table 1. Variables and Parameters Descriptions

Variables/Parameters	Descriptions	Parameter Units
$\boldsymbol{L(t)}$	Concentration of Aluminum 5083 undergoing corrosion	$Concentration$
$\boldsymbol{N(t)}$	Concentration of corrosive ions formed during the corrosion process	$Concentration$
$\boldsymbol{K(t)}$	Concentration of corrosion products resulting from the reaction between aluminum and corrosive ions	$Concentration$
$\boldsymbol{O(t)}$	Concentration of oxygen involved in the corrosion process	$Concentration$
$\boldsymbol{C(t)}$	Concentration of chloride ions involved in the corrosion process	$Concentration$
$\boldsymbol{P(t)}$	Concentration of the passivation layer formed	$Concentration$
$\boldsymbol{\varepsilon}$	Effectiveness level of the protective layer	$-$
$\boldsymbol{k_1}$	Reaction rate coefficient for aluminum and corrosive ions	$\frac{1}{time}$
$\boldsymbol{k_2}$	Reaction coefficient of Aluminum with oxide ions	$\frac{1}{time}$
$\boldsymbol{k_3}$	Generation rate coefficient of corrosive intermediates due to aluminum dissolution.	$\frac{1}{time}$
$\boldsymbol{k_4}$	Natural decay or neutralization rate coefficient of corrosive species	$\frac{1}{time}$
$\boldsymbol{k_5}$	Reaction coefficient describing the consumption of corrosive ions during corrosion product formation involving aluminum.	$\frac{1}{time \times concentration}$
$\boldsymbol{k_6}$	Production rate coefficient of corrosion products K from the interaction between aluminum and corrosive ions.	$\frac{1}{time \times concentration}$
$\boldsymbol{k_7}$	Reaction coefficient of Aluminum with chloride ions	$\frac{1}{time}$
$\boldsymbol{k_8}$	Reaction coefficient for the formation of the passivation layer from the reaction between Aluminum and Oxygen	$\frac{1}{time \times concentration}$
$\boldsymbol{k_9}$	Natural degradation coefficient of the passive layer	$\frac{1}{time}$
$\boldsymbol{k_{10}}$	Protection coefficient against corrosive ions (Chloride)	$\frac{1}{time \times concentration}$
$\boldsymbol{k_{11}}$	Degradation coefficient of corrosion products	$\frac{1}{time}$
$\boldsymbol{k_{12}}$	Oxygen consumption coefficient associated with aluminum oxidation processes.	$\frac{1}{time \times concentration}$
$\boldsymbol{k_{13}}$	Effective chloride consumption coefficient near the surface during corrosion and film interaction.	$\frac{1}{time \times concentration}$
$\boldsymbol{D_c}$	Diffusion coefficient of chloride ions	$\frac{1}{time}$
$\boldsymbol{D_o}$	Diffusion coefficient of oxygen	$\frac{1}{time}$

Furthermore, the mathematical model in this study will be formulated using a system of fractional differential equations. Subsequently, stability analysis of the equilibrium points for the fractional differential equation system will be conducted. Numerical simulations will be performed using MATLAB software with the PECE-PI method to predict system behavior under various conditions. The obtained results will then be analyzed to gain insight into the dynamics of corrosion behavior.

3. RESULTS AND DISCUSSION

3.1 Proposed Fractional Mathematical Model and Non-Negativity Analysis

The model in Eq. (5) represents the corrosion rate model formulated using ordinary integer-order differential equations. This study will focus on models employing systems of fractional differential equations (FDEs). Therefore, the model in Eq. (5) is transformed into a system of fractional-order differential equations (SFDE) utilizing the Caputo fractional derivative definition as follows:

$$\begin{aligned}
\frac{1}{\sigma^{1-\alpha}}\,{}_0^cD_t^\alpha L(t) &= -f(P)[k_1LN + k_2LO + k_7LC],\\
\frac{1}{\sigma^{1-\alpha}}\,{}_0^cD_t^\alpha N(t) &= k_3L - k_4N - k_5LN,\\
\frac{1}{\sigma^{1-\alpha}}\,{}_0^cD_t^\alpha K(t) &= k_6NL - k_{11}K,\\
\frac{1}{\sigma^{1-\alpha}}\,{}_0^cD_t^\alpha O(t) &= \widetilde{D}_0(O_{env} - O) - k_{12}LO,\\
\frac{1}{\sigma^{1-\alpha}}\,{}_0^cD_t^\alpha C(t) &= \widetilde{D}_c(C_{env} - C) - k_{13}LC - k_{10}CP,\\
\frac{1}{\sigma^{1-\alpha}}\,{}_0^cD_t^\alpha P(t) &= k_8LO - k_9P - k_{10}CP.
\end{aligned} \tag{11}$$

The substitution of the integer-order derivative on the left-hand side of the model in Eq. (5) with the Caputo fractional derivative in the model in Eq. (11) results in a dimensional change in the time variable t. An integer-order derivative operator $\frac{d}{dt}$ possesses the dimension of s^{-1}, whereas the Caputo fractional derivative $\frac{d^\alpha}{dt^\alpha} = {}_0^cD_t^\alpha$ has the dimension $s^{-\alpha}$, with $0 < \alpha \leq 1$ [6]. To accommodate this dimensional modification on the left side of Eq. (11), we introduce the new scale parameter σ, where $\frac{1}{\sigma^{1-\alpha}}$ has the dimension $s^{1-\alpha}$. This scaling parameter ensures that Eq. (11) remains dimensionally consistent (dimensionally compatible). Furthermore, it will be demonstrated that the solution to system Eq. (11) is non-negative. This property is essential given that the model deals with chemical reaction processes, where physical concentrations must be non-negative. The positivity of the solution indicates that the state variables $\{L, N, K, O, C, P\}$ remain non-negative within the domain of definition. To guarantee this, the following lemma is stated.

Lemma 1. *Suppose the initial values satisfy* $\{L_0, N_0, K_0, O_0, C_0, P_0 \geq 0\} \in \Omega$. *Then, the solution set* $\{L, N, K, O, C, P\}$ *of system Eq. (11) is non-negative for all* $t > 0$.

Proof. From the first equation of system Eq. (11), we have

$$\begin{aligned}
{}_0^CD_t^\alpha L(t) &= -f(P)(k_1^\alpha LN + k_2^\alpha LO + k_7^\alpha LC),\\
&= -f(P)(k_1^\alpha N + k_2^\alpha O + k_7^\alpha C)L,\\
&\geq -(k_1^\alpha + k_2^\alpha + k_7^\alpha)L,\\
&\geq -M_1L,
\end{aligned}$$

which satisfies ${}_0^CD_t^\alpha L(t) \geq -M_1L$.

Applying the basic comparison theorem for fractional order differential equations [26], it follows that

$$\begin{aligned}
L &\geq L(0)E_\alpha(-M_1t^\alpha),\\
L &\geq L(0)E_\alpha(-M_1t^\alpha) \geq 0,
\end{aligned}$$

where $E_\alpha(\cdot)$ denotes the Mittag-Leffler function. Due to the positivity property of the Mittag-Leffler function for $\alpha \in (0,1)$[27]**.** By analogous reasoning, the non-negativity of the other state variables is established:

$$N \geq 0, K \geq, O \geq 0, C \geq 0, P \geq 0.$$

Therefore, the solution to system Eq. (11) remains non-negative in Ω, proving that it is physically meaningful within the model's domain. ■

3.2 Equilibrium Points of the Fractional Model

Determining the equilibrium points in model Eq. (11) is essential to identifying solutions that remain constant over time t. These equilibrium points can be found by solving the following system of equations derived from setting the fractional derivatives to zero:

$$ {}_0^cD_t^\beta L(t) = {}_0^cD_t^\beta N(t) = {}_0^cD_t^\beta K(t) = {}_0^cD_t^\beta O(t) = {}_0^cD_t^\beta C(t) = {}_0^cD_t^\beta P(t) = 0.$$

Thus, the equilibrium points of the system are

$$L^* = 0, N^* = 0, K^* = 0, O^* = O_{env}, C_l^* = C_{env}, P^* = 0.$$

3.3 Sensitivity Analysis and Stability Analysis

In corrosion rate modelling, one important aspect to examine is the effort to control corrosion by considering the contribution of parameters within the model. To evaluate the significance of parameter variations on a specific variable, sensitivity analysis can be conducted. Sensitivity measures the relative change in a variable in response to changes in a parameter. In this section, the results of the sensitivity analysis for each parameter are presented with respect to the concentration variables of Aluminum (L), corrosive ion (N), and corrosion product (K), using the *Latin Hypercube Sampling-Partial Rank Correlation Coefficients* (LHS-PRCC) method.

Based on Fig. 1 – Fig. 3, the sensitivity analysis results reveal the influence of each parameter on the concentration changes of the three model variables: the concentration of aluminum 5083 (L), the concentration of corrosive ions (N), and the concentration of corrosion products (K). Parameters that directly contribute to the model exhibit higher PRCC values. PRCC values with larger magnitudes indicate that the corresponding parameter exerts a strong monotonic influence on changes in the output variable, while the sign of the PRCC reflects the direction of this relationship. However, in addition to the directly influencing parameters, other parameters also affect the concentrations of each variable

Fig. 1 illustrates the PRCC values of all model parameters with respect to changes in the aluminum concentration. Parameters k_1, k_2 and k_7 exhibit the most dominant PRCC values among the considered parameters. The negative PRCC values associated with these parameters indicate that increasing their respective values leads to a decrease in the aluminum concentration. Moreover, the magnitudes of these PRCC values exceed 0.7, suggesting a strong physical influence on variations in the aluminum concentration. Fig. 2 presents the PRCC values of all parameters with respect to changes in the concentration of corrosive ions. In this simulation, three parameters k_3, k_4 and k_5. show dominant amplitudes. In contrast to the previous case, not all dominant parameters exhibit negative PRCC values. Parameter k_3 has a PRCC value of approximately +0.9, indicating that an increase in k_3 significantly raises the concentration of corrosive ions. Conversely, parameters k_4 and k_5 display negative PRCC values of about −0.6 and −1, respectively, implying that increases in these parameters result in a reduction of the corrosive ion concentration in the model.

Finally, Fig. 3 depicts the PRCC-based sensitivity analysis of the corrosion product concentration with respect to all model parameters. The parameter with the largest amplitude is k_6, with a PRCC value close to +1, indicating that higher values of k_6 lead to a greater production of corrosion products. In contrast, two significant parameters yield negative PRCC values, namely k_5 and k_7, with values of approximately −0.6 and −0.5, respectively. This indicates that increasing these parameters results in a decrease in the concentration of corrosion products predicted by the model. Fig. 4 – Fig. 6 display plots demonstrating the relationships for each significant parameter pair concerning the concentration of aluminum 5083 metal. The simulation results indicate that a lower combined reaction rate between two parameters can reduce the rate of change in aluminum 5083 concentration. In other words, by slowing down the reaction rate between aluminum 5083 metal and corrosive ions, the decrease in aluminum metal concentration can be slowed.

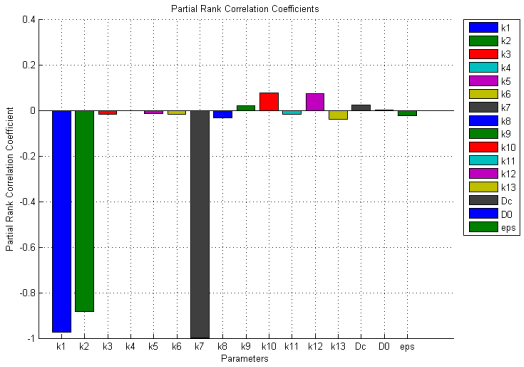

Figure 1. PRCC Statistics Regarding the Significance of Factors Associated with L

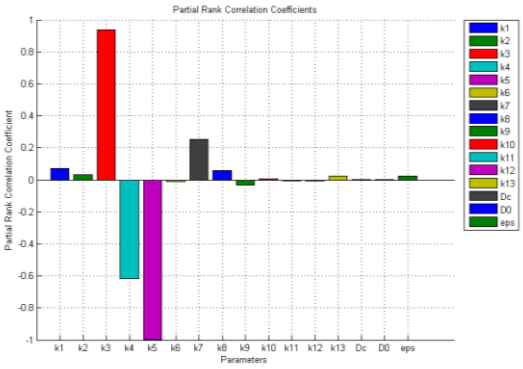

Figure 2. PRCC Statistics Regarding the Significance of Factors Associated with N

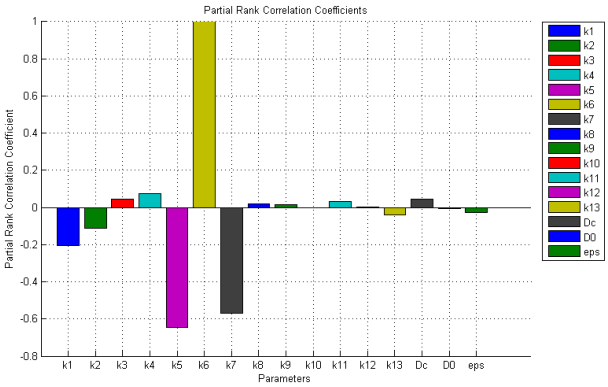

Figure 3. PRCC Statistics Regarding the Significance of Factors Associated with K

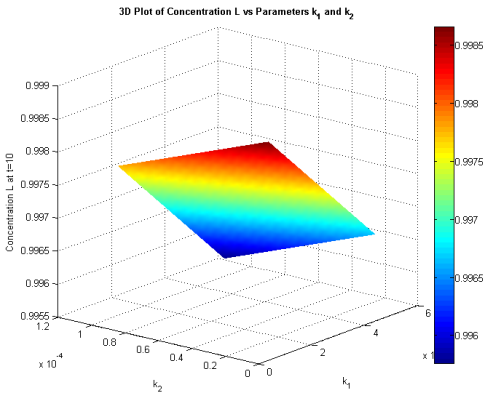

Figure 4. The Behavior of L with k_1 vs k_2 Parameters

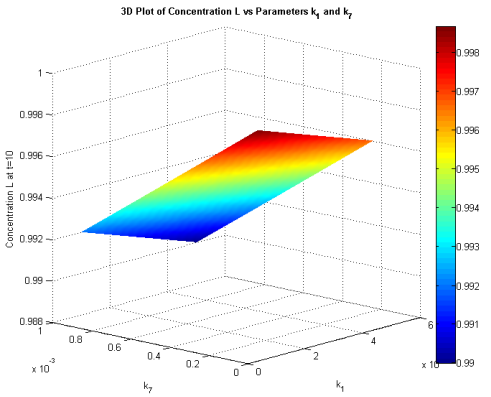

Figure 5. The Behaviour of L with k_1 vs k_7 Parameters

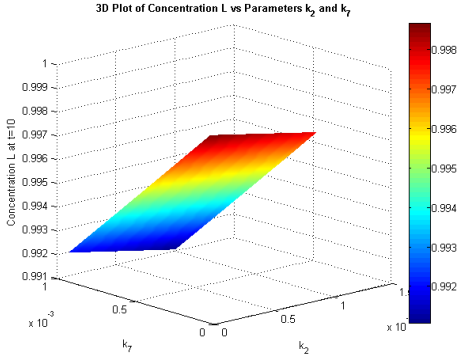

Figure 6. The Behavior of L with k_2 vs k_7 Parameters

Based on Theorem 1 and Theorem 2, an equilibrium point $\bar{\boldsymbol{x}}$ is said to be locally asymptotically stable if all eigenvalues $\lambda_j, j = 1,2,\dots,n$ of the Jacobian matrix satisfy the condition $\left|\arg(\lambda_j)\right| > \frac{\alpha\pi}{2}$. If the system in Eq. (11) is linearized, the resulting Jacobian matrix is obtained as follows:

$$J = \begin{pmatrix} \frac{-k_1^\alpha N - k_2^\alpha O - k_7^\alpha C}{1+\varepsilon P} & -\frac{k_1^\alpha L}{1+\varepsilon P} & 0 & -\frac{k_2^\alpha L}{1+\varepsilon P} & -\frac{k_7^\alpha L}{1+\varepsilon P} & \frac{\varepsilon}{(1+\varepsilon P)^2}(k_1^\alpha LN + k_2^\alpha LO + k_7^\alpha LC) \\ k_3^\alpha - k_5^\alpha N & -k_4^\alpha - k_5^\alpha L & 0 & 0 & 0 & 0 \\ k_6^\alpha N & k_6^\alpha L & -k_{11}^\alpha & 0 & 0 & 0 \\ -k_{12}^\alpha O & 0 & 0 & -D_o^\alpha - k_{12}^\alpha L & 0 & 0 \\ -k_7^\alpha L & 0 & 0 & 0 & -D_c^\alpha - k_{13}^\alpha L - k_{10}^\alpha P & -k_{10}^\alpha C \\ k_8^\alpha O & 0 & 0 & k_8^\alpha L & -k_{10}^\alpha P & -k_9^\alpha - k_{10}^\alpha C \end{pmatrix}.$$

By substituting the equilibrium point, we obtain

$$J = \begin{pmatrix} -k_2^\alpha O_{env} - k_7^\alpha C_{env} & 0 & 0 & 0 & 0 & 0 \\ k_3^\alpha & -k_4^\alpha & 0 & 0 & 0 & 0 \\ 0 & 0 & -k_{11}^\alpha & 0 & 0 & 0 \\ -k_{12}^\alpha O_{env} & 0 & 0 & -D_o^\alpha & 0 & 0 \\ 0 & 0 & 0 & 0 & -D_c^\alpha & -k_{10}^\alpha C_{env} \\ k_8^\alpha O_{env} & 0 & 0 & 0 & 0 & -k_9^\alpha - k_{10}^\alpha C_{env} \end{pmatrix}. \quad (12)$$

Based on the Jacobian matrix, the characteristic equation is obtained as

$$(\lambda + k_{11}^\alpha)(\lambda + D_o^\alpha)(\lambda + k_4^\alpha)(\lambda + k_9^\alpha + k_{10}^\alpha C_{env})(\lambda + k_2^\alpha O_{env} + k_7^\alpha C_{env})(\lambda + D_c^\alpha) = 0. \quad (13)$$

From the characteristic Eq. (13), the eigenvalues are

$$\lambda_1 = -k_{11}^\alpha,$$
$$\lambda_2 = -D_o^\alpha,$$
$$\lambda_3 = -k_4^\alpha,$$
$$\lambda_4 = -k_9^\alpha - k_{10}^\alpha C_{env},$$
$$\lambda_5 = -k_2^\alpha O_{env} - k_7^\alpha C_{env},$$
$$\lambda_6 = -D_c^\alpha.$$

Since all model parameters are positive, it follows that $\lambda_i < 0$ for all $i = 1,\dots,6$. In other words, $\left|\arg(\lambda_i)\right| = \pi$. Thus for $0 < \alpha < 1$ it can be assured that $\left|\arg\left(\lambda_{1,\dots,6}\right)\right| > \frac{\alpha\pi}{2}$. In other words, the local asymptotic stability indicates that the corrosion system naturally approaches a steady state, suggesting that the material's corrosion rate will stabilize over long-term exposure.

3.4 Numerical Simulation and Discussion

Numerical simulations are conducted to examine the system's behavior over a specified time interval, providing insights into the dynamics of interactions occurring during the corrosion process. By assigning values to the model parameters and initial conditions for each variable, and subsequently modifying certain parameters, the resulting changes in the model dynamics can be observed. We assume the initial parameter values used for the simulation, along with the initial values of each variable, are presented in Table 2. In this numerical simulation, the system in Eq. (11) is transformed into the numerical schemes given in Eqs. (3) and (4) using the PECE-PI method. The simulation aims to investigate the dynamics of each model variable by considering four different fractional orders, namely $\alpha = 0.65; 0.75; 0.85$ and 0.95. Through this approach, differences in the behavior of each variable under varying fractional orders can be clearly observed.

Table 2. Parameters Values

Variables/Parameters	Value	Variables/Parameters	Value
$\boldsymbol{L(t)}$	$1\ M$	k_4	$1\times10^{-7} - 5\times10^{-6}$
$\boldsymbol{N(t)}$	$0.5\ M$	k_5	$1\times10^{-4} - 1\times10^{-3}$
$\boldsymbol{K(t)}$	$0\ M$	k_6	$1\times10^{-4} - 5\times10^{-4}$
$\boldsymbol{O(t)}$	$0.2\ M$	k_7	$1\times10^{-4} - 1\times10^{-3}$
$\boldsymbol{C(t)}$	$0.1\ M$	k_8	$1\times10^{-5} - 1\times10^{-4}$

Variables/Parameters	Value	Variables/Parameters	Value
$\boldsymbol{P(t)}$	$0.05\ M$	k_9	$1\times10^{-7}-1\times10^{-6}$
$\boldsymbol{\varepsilon}$	$0-1$	k_{10}	$1\times10^{-7}-1\times10^{-6}$
$\boldsymbol{k_1}$	$1\times10^{-4}-5\times10^{-4}$	k_{11}	$1\times10^{-7}-1\times10^{-6}$
$\boldsymbol{k_2}$	$1\times10^{-5}-1\times10^{-4}$	D_c	$(1-2)\times10^{-9}$
$\boldsymbol{k_3}$	$1\times10^{-6}-1\times10^{-5}$	D_0	$(2-3)\times10^{-9}$

Fig. 7 – Fig. 12 illustrate the dynamics of each model variable through simulations conducted at various fractional orders. Throughout the simulation duration, the total concentration of Aluminum 5083 exhibits an overall decline. As shown in Fig. 7, among the four simulated fractional-order values, $\alpha = 0.95$ demonstrates a most rapid decrease in concentration compared to the other orders. The simulation results indicate that the aluminum concentration decreases by approximately 0.9% within 200 hours for $\alpha = 0.95$, whereas the reduction is about 0.2% for $\alpha = 0.65$. Furthermore, with lower fractional orders, the decline in concentration is noticeably slower. This suggests that increasing the fractional order α accelerate the system's progression toward a steady state. Fig. 8 presents the simulation results for the corrosive ion concentration variable. The simulations indicate a general decline in concentration across all fractional order values tested. Notably, the fractional order $\alpha = 0.95$ exhibits the fastest decrease in corrosive ion concentration compared to other fractional orders, which decrease approximately 1.6% within 200 hours.

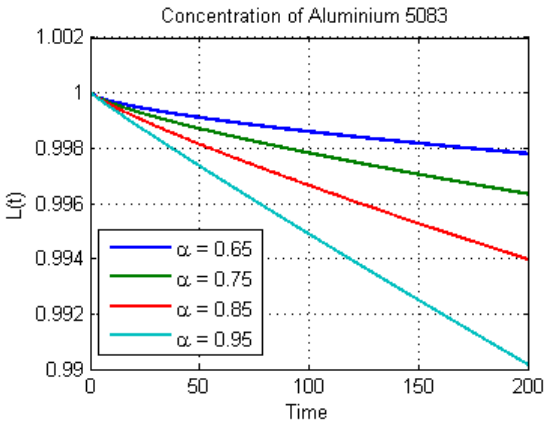

Figure 7. The Dynamics of Aluminum Concentration

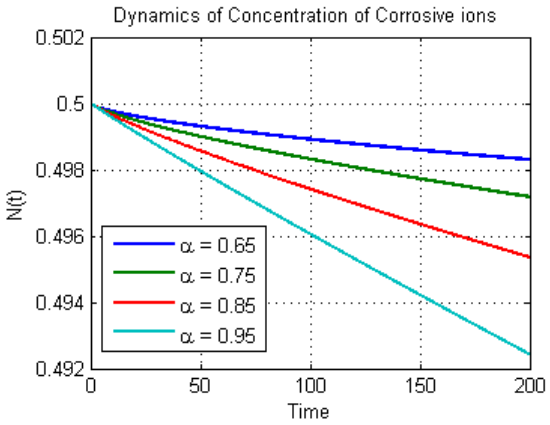

Figure 8. The Dynamics of Ionic Corrosion Concentration

Fig. 9 and Fig.10, which represent the dynamics of chloride ion and oxygen concentrations, respectively, display similar behavior patterns. As the fractional order decreases, the rate of concentration decline for each variable slows. These observations suggest a deceleration in the reaction rates between chloride ions and oxygen with aluminum during the corrosion process. Fig.11 shows the dynamics of corrosion product concentration with 100 hours of simulation. This result indicates that $\alpha = 0.95$ also depicts the highest increase for reaching 0.008 M at the end of the simulation, which is four times faster than the corrosion product concentration at $\alpha = 0.65$. Additionally, Fig. 12 depicts the passivation layer concentration. The concentration of the passivation layer increases as the metal bonds with oxygen, forming a protective layer that shields the aluminum from corrosion attack. The simulation results over a 200-hour period show that $\alpha = 0.95$ produces a slightly higher increase in the concentration of the passivation layer compared to the other fractional orders.

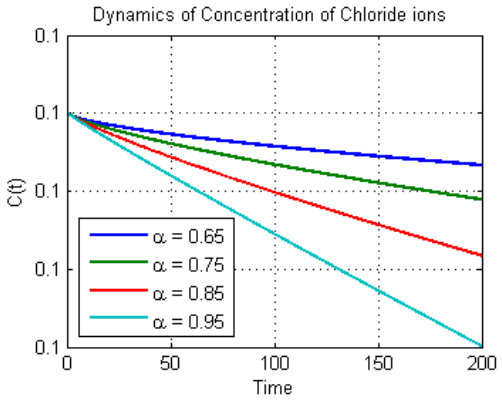

Figure 9. The Dynamics of Chloride Concentration

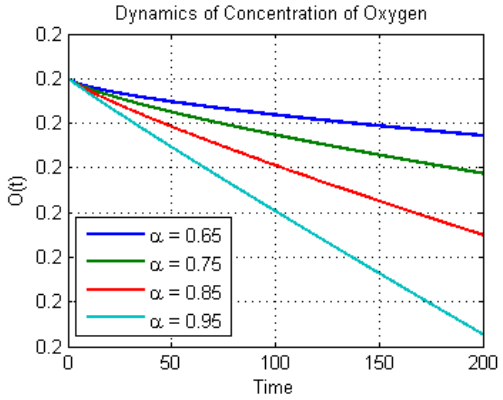

Figure 10. The Dynamics of Oxygen Concentration

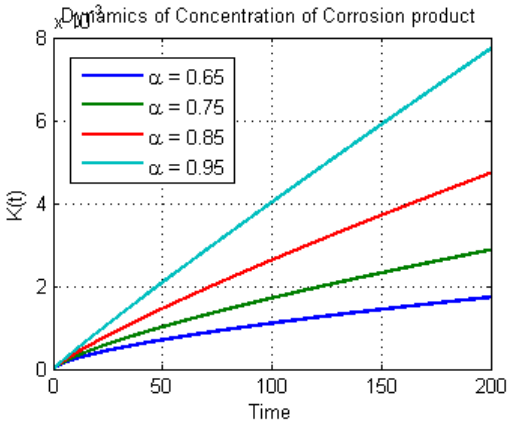

Figure 11. The Dynamics of Corrosion Product Concentration

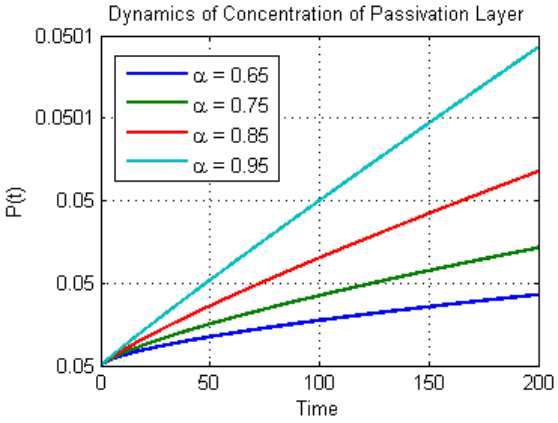

Figure 12. The Dynamics of Passivation Concentration

In general, varying fractional orders significantly affect the rates of decrease and increase in the concentrations of each variable. Simulation results show that smaller fractional order values α correspond to a deceleration in both decreasing and increasing behaviors of the concentrations. This phenomenon indicates that lower fractional orders α implies that the system exhibits stronger memory effects or a higher degree of inertia, whereby changes such as decay do not occur abruptly but rather progress gradually due to the influence of the system's memory. The simulation results obtained in this study exhibit behavior consistent with previous simulation-based research conducted by Fajri et al.[2] in which the concentration of aluminum metal decreases over the simulation interval. On the other hand, the decline in aluminum concentration accompanied by an increase in corrosion products is in line with the experimental findings reported by Huda and Suthajo [3], thereby validating the results obtained in the present study.

4. CONCLUSION

This study provides the first fractional differential framework for modeling Aluminum 5083 corrosion, offering a new approach for predicting material degradation in marine engineering. The conclusions of this study are:

1. Stability analysis of the model indicates the presence of a locally asymptotically stable equilibrium point, with all eigenvalues satisfying $\left|\arg(\lambda)\right| > \frac{\alpha\pi}{2}$.

2. Sensitivity analysis identifies key parameters significantly influencing the concentration changes of aluminum, corrosive ions, and corrosion products. Numerical simulations yield outcomes consistent with observed field phenomena, where concentrations of aluminum, corrosive ions, chloride, and oxygen decrease, while concentrations of corrosion products and the passivation layer increase.

3. By employing fractional-order modelling, the fractional order α reveals a memory effect that influences the rate of concentration increase and decrease of each variable. A smaller fractional order α corresponds to a stronger memory effect, enabling a deceleration in the decay processes.

This model provides an insightful visualization of corrosion processes occurring on aluminum, particularly for ship materials. The current study is limited to model development and numerical simulations to present initial findings. To enhance model accuracy, especially for predictive purposes, future research should focus on experimental validation to obtain more realistic parameter estimations. Furthermore, integrating additional variables not currently considered in this model (such as temperature and pH) could enrich the analysis results. Such enhancements will improve the model's utility as a decision-making guide in ship material planning and maintenance, increasing efficiency in mitigation efforts to support operational safety in harsh marine environments.

Author Contributions

Muhammad Rifki Nisardi: Writing – Original Draft, Visualization, Validation, Software, Methodology, Investigation, Formal Analysis. Nur Rahmi: Writing – Original Draft, Validation, Formal Analysis, Data Curation. Muhammad Akram Arifuddin: Literature Review, Project Administration, Data Curation. Hartina Husain: Validation, Methodology, Data Curation. Kusnaeni: Visualization, Project Administration, Methodology. All authors discussed the results and contributed to the final manuscript.

Funding Statement

This work was supported by the Ministry of Higher Education, Science, and Technology (Kemdiktisaintek) (No. 014/C3/DT.05.00/PL/2025) under Penelitian Dosen Pemula (PDP) 2025 BIMA grant scheme.

Acknowledgment

The authors gratefully acknowledge the insightful comments and constructive feedback provided by the reviewers. Their careful evaluation and thoughtful suggestions have substantially contributed to the improvement of this work.

Declarations

The authors declare that they have no known competing financial interests or personal relationships that could have appeared to influence the work reported in this paper.

Declaration of Generative AI and AI-Assisted Technologies

Generative AI tools (e.g., ChatGPT) were used solely for language refinement, including grammar, spelling, and clarity. The scientific content, analysis, interpretation, and conclusions were developed entirely by the authors. All final text was reviewed and approved by the authors.

REFERENCES

[1] S. Prasetyo, U. Budiarto, W. Amiruddin, and J. Soedarto, "ANALISA LAJU KOROSI PADA MATERIAL ALUMINIUM 5083 MENGGUNAKAN MEDIA AIR LAUT SEBAGAI APLIKASI BAHAN LAMBUNG KAPAL," vol. 7, no. 4, 2019.

[2] K. Fajri, H. Misni, and M. Triwahyu, "PENGEMBANGAN MODEL MATEMATIKA LAJU KOROSI ALUMINIUM 5083 PADA KAPAL CEPAT RUDAL 60 METER," *Jurnal Sains dan Teknologi Maritim (JSTM)*, vol. 25, no. 2, pp. 201–214, Mar. 2025. doi: https://doi.org/10.33556/jstm.v25i2.460

[3] C. Huda and D. H. Sutjahjo, "ANALISIS LAJU KOROSI MATERIAL ALUMINIUM 5083 SEBAGAI APLIKASI BAHAN LAMBUNG KAPAL," *JPTM*, vol. 06, no. 2, pp. 17–24, 2017.

[4] D. Agustini and L. Fitriah, "PEMODELAN MATEMATIKA PADA SISTEM KOROSI LOGAM," *Lombok Journal of Science (LJS)*, vol. 5, no. 1, 2023.

[5] R. E. Maghfiroh, M. L. Dewi, and R. Khusniah, "MATHEMATICAL MODEL OF METAL CORROSION RATE WITH ENVIRONMENTAL FACTORS THAT SPEED UP CORROSION," *map*, vol. 6, no. 1, pp. 1–7, June 2024. doi: https://doi.org/10.15548/map.v6i1.7277

[6] L. C. de Barros, M. M. Lopes, F. S. Pedro, E. Esmi, J. P. C. dos Santos, and D. E. Sánchez, "THE MEMORY EFFECT ON FRACTIONAL CALCULUS: AN APPLICATION IN THE SPREAD OF COVID-19," *Comp. Appl. Math.*, vol. 40, no. 3, p. 72, Apr. 2021. doi: https://doi.org/10.1007/s40314-021-01456-z

[7] A. Atangana and S. İ. Araz, "FRACTIONAL STOCHASTIC MODELLING ILLUSTRATION WITH MODIFIED CHUA ATTRACTOR," *Eur. Phys. J. Plus*, vol. 134, no. 4, p. 160, Apr. 2019. doi: https://doi.org/10.1140/epjp/i2019-12565-6

[8] E. Bas, B. Acay, and R. Ozarslan, "FRACTIONAL MODELS WITH SINGULAR AND NON-SINGULAR KERNELS FOR ENERGY EFFICIENT BUILDINGS," *Chaos: An Interdisciplinary Journal of Nonlinear Science*, vol. 29, no. 2, p. 23110, 2019. doi: https://doi.org/10.1063/1.5082390

[9] R. Huang and Y. Pu, "A NOVEL FRACTIONAL MODEL AND ITS APPLICATION IN NETWORK SECURITY SITUATION ASSESSMENT," *Fractal Fract*, vol. 8, no. 10, p. 550, Sept. 2024. doi: https://doi.org/10.3390/fractalfract8100550

[10] D. Kumar, H. Nama, and D. Baleanu, "NUMERICAL AND COMPUTATIONAL ANALYSIS OF FRACTIONAL ORDER MATHEMATICAL MODELS FOR CHEMICAL KINETICS AND CARBON DIOXIDE ABSORBED INTO PHENYL GLYCIDYL ETHER," *Results in Physics*, vol. 53, p. 107003, Oct. 2023. doi: https://doi.org/10.1016/j.rinp.2023.107003

[11] M. R. Nisardi, K. Kasbawati, and K. Khaeruddin, "A MATHEMATICAL MODEL ANALYSIS OF COVID-19 TRANSMISSION WITH VACCINATION IN CAPUTO FRACTIONAL DERIVATIVES: CASE STUDY IN INDONESIA," *JTAM*, vol. 8, no. 4, p. 1183, Oct. 2024. doi: https://doi.org/10.31764/jtam.v8i4.24711

[12] L.-J. Shen, "FRACTIONAL DERIVATIVE MODELS FOR VISCOELASTIC MATERIALS AT FINITE DEFORMATIONS," *International Journal of Solids and Structures*, vol. 190, pp. 226–237, May 2020. doi: https://doi.org/10.1016/j.ijsolstr.2019.10.025

[13] B. Díaz, B. Grgur, and J. Wang, "CURRENT CHALLENGES IN CORROSION RESEARCH," *Metals*, vol. 14, no. 10, p. 1194, Oct. 2024. doi: https://doi.org/10.3390/met14101194

[14] K. V. Akpanyung and R. T. Loto, "PITTING CORROSION EVALUATION: A REVIEW," *J. Phys.: Conf. Ser.*, vol. 1378, no. 2, p. 022088, Dec. 2019. doi: https://doi.org/10.1088/1742-6596/1378/2/022088

[15] M. Schneider, K. Kremmer, C. Lämmel, K. Sempf, and M. Herrmann, "GALVANIC CORROSION OF METAL/CERAMIC COUPLING," *Corrosion Science*, vol. 80, pp. 191–196, Mar. 2014. doi: https://doi.org/10.1016/j.corsci.2013.11.024

[16] K. Zhang, E. Rahimi, N. Van Den Steen, H. Terryn, A. Mol, and Y. Gonzalez-Garcia, "MONITORING ATMOSPHERIC CORROSION UNDER MULTI-DROPLET CONDITIONS BY ELECTRICAL RESISTANCE SENSOR MEASUREMENT," *Corrosion Science*, vol. 236, p. 112271, Aug. 2024. doi: https://doi.org/10.1016/j.corsci.2024.112271

[17] X. Hou, L. Gao, Z. Cui, and J. Yin, "CORROSION AND PROTECTION OF METAL IN THE SEAWATER DESALINATION," *IOP Conf. Ser.: Earth Environ. Sci.*, vol. 108, p. 022037, Jan. 2018. doi: https://doi.org/10.1088/1755-1315/108/2/022037

[18] G.-G. Kim, D.-Y. Kim, I. Hwang, D. Kim, Y.-M. Kim, and J. Park, "MECHANICAL PROPERTIES OF ALUMINUM 5083 ALLOY GMA WELDS WITH DIFFERENT MAGNESIUM AND MANGANESE CONTENT OF FILLER WIRES," *Applied Sciences*, vol. 11, no. 24, p. 11655, Dec. 2021. doi: https://doi.org/10.3390/app112411655

[19] Y. Li *et al.*, "THE CORROSION BEHAVIOR AND MECHANICAL PROPERTIES OF 5083 AL-MG ALLOY MANUFACTURED BY ADDITIVE FRICTION STIR DEPOSITION," *Corrosion Science*, vol. 213, p. 110972, 2023. doi: https://doi.org/10.1016/j.corsci.2023.110972

[20] M. S. Tavazoei and M. Haeri, "A NECESSARY CONDITION FOR DOUBLE SCROLL ATTRACTOR EXISTENCE IN FRACTIONAL-ORDER SYSTEMS," *Physics Letters A*, vol. 367, no. 1–2, pp. 102–113, July 2007. doi: https://doi.org/10.1016/j.physleta.2007.05.081.

[21] D. Pang, W. Jiang, and A. U. K. Niazi, "FRACTIONAL DERIVATIVES OF THE GENERALIZED MITTAG-LEFFLER FUNCTIONS," *Adv Differ Equ*, vol. 2018, no. 1, Dec. 2018. doi: https://doi.org/10.1186/s13662-018-1855-9

[22] D. Matignon, "STABILITY RESULTS FOR FRACTIONAL DIFFERENTIAL EQUATIONS WITH APPLICATIONS TO CONTROL PROCESSING," vol. 2, Jan. 1997.

[23] E. Ahmed, A. El-Sayed, and H. El-Saka, "ON SOME ROUTH-HURWITZ CONDITIONS FOR FRACTIONAL ORDER DIFFERENTIAL EQUATIONS AND THEIR APPLICATIONS IN LORENZ, RÖSSLER, CHUA AND CHEN SYSTEMS," *Physics Letters A*, vol. 358, no. 1, pp. 1–4, Jan. 2006. doi: https://doi.org/10.1016/j.physleta.2006.04.087

[24] R. Garrappa, "NUMERICAL SOLUTION OF FRACTIONAL DIFFERENTIAL EQUATIONS: A SURVEY AND A SOFTWARE TUTORIAL," *Mathematics*, vol. 6, no. 2, p. 16, Jan. 2018. doi: https://doi.org/10.3390/math6020016

[25] J. Jaume, M. J. F. Marques, M. L. Délia, and R. Basséguy, "SURFACE MODIFICATION OF 5083 ALUMINUM-MAGNESIUM INDUCED BY MARINE MICROORGANISMS," *Corrosion Science*, vol. 194, p. 109934, 2022. doi: https://doi.org/10.1016/j.corsci.2021.109934.

[26] S. S. Askar, D. Ghosh, P. K. Santra, A. A. Elsadany, and G. S. Mahapatra, "A FRACTIONAL ORDER SITR MATHEMATICAL MODEL FOR FORECASTING OF TRANSMISSION OF COVID-19 OF INDIA WITH LOCKDOWN EFFECT," *Results in Physics*, vol. 24, p. 104067, May 2021. doi: https://doi.org/10.1016/j.rinp.2021.104067

[27] Z. Wei, Q. Li, and J. Che, "INITIAL VALUE PROBLEMS FOR FRACTIONAL DIFFERENTIAL EQUATIONS INVOLVING RIEMANN–LIOUVILLE SEQUENTIAL FRACTIONAL DERIVATIVE," *Journal of Mathematical Analysis and Applications*, vol. 367, no. 1, pp. 260–272, July 2010. doi: https://doi.org/10.1016/j.jmaa.2010.01.023